



## Evidence for rainfall-triggered earthquake activity

S. Hainzl,<sup>1</sup> T. Kraft,<sup>2</sup> J. Wassermann,<sup>2</sup> H. Igel,<sup>2</sup> and E. Schmedes<sup>2</sup>

Received 21 July 2006; revised 24 August 2006; accepted 30 August 2006; published 5 October 2006.

[1] Fluids are known to be of major importance for the earthquake generation because pore pressure variations alter the strength of faults. Thus they can initiate earthquakes if the crust is close enough to its critical state. Based on the observations of the isolated seismicity below the densely monitored Mt. Hochstaufen, SE Germany, we are now able to demonstrate that the crust can be so close-to-failure that even tiny pressure variations associated with precipitation can trigger earthquakes in a few kilometer depth. We find that the recorded seismicity is highly correlated with the calculated spatiotemporal pore pressure changes due to diffusing rain water and in good agreement with the response of faults described by the rate-state friction law. **Citation:** Hainzl, S., T. Kraft, J. Wassermann, H. Igel, and E. Schmedes (2006), Evidence for rainfall-triggered earthquake activity, *Geophys. Res. Lett.*, 33, L19303, doi:10.1029/2006GL027642.

### 1. Introduction

[2] In recent years, hydromechanical coupling has been proposed as a possible explanation for many geological phenomena including the anomalous weakness of many major faults [Sleep and Blanpied, 1992], silent slip events [Kodaira et al., 2004], aftershock occurrence [Nur and Booker, 1972; Miller et al., 2004], and remote triggering of earthquakes [Prejean et al., 2004]. The widely accepted understanding is that an increase of the pore fluid pressure reduces the effective normal stress and thus the strength of faults, promoting earthquake rupture. Direct evidence for fluids affecting the stability of faults comes from reservoir induced seismicity [Talwani, 1997], and fluid injections in wells [Zoback and Harjes, 1997]. Fluid triggering is also observed for natural seismicity such as earthquake swarms where the fluid source is assumed to be in depth [Parotidis et al., 2003; Miller et al., 2004; Hainzl and Ogata, 2005]. Furthermore, seasonal variations of the seismic activity have been found which seems to correlate with the seasonality of ground water recharge [Saar and Manga, 2003] and precipitation [Muco, 1999]. However, so far, the lack of high-resolution data did not allow to prove the effect of surface water in more detail. Based on our observations for the isolated seismicity below Mt. Hochstaufen, we are now able to show that rainfall can trigger earthquakes via the mechanism of pore pressure diffusion.

### 2. Seismicity at Mt. Hochstaufen

[3] The Staufen Massif is an east-west striking mountain chain in SE Germany, northwest of the town Bad Reich-

enhall. The most prominent summit, Mt. Hochstaufen, reaches an altitude of 1775m (Figure 1). Belonging to the elongated fold-and-thrust belt of the Northern Limestone Alps, the geology of the Staufen Massif is dominated by lower to middle Triassic limestone and dolomite [Bögel and Schmidt, 1976]. Since more than 600 years ago, earthquakes with maximum macroseismic intensities of  $I_0 = V$  have been reported in this region, which is embedded in an almost quiet surrounding. The majority of the earthquakes occurs in the summer months, which are also characterized by having the highest average precipitation values during the year [Kraft et al., 2006a]. To explore the underlying mechanisms, seismic monitoring of the Bad Reichenhall area was initiated in 2001, consisting of six permanent and three mobile short period stations (see locations in Figure 1). In 2002, this network recorded more than 1100 earthquakes with a maximum magnitude of  $M_l = 2.4$ , mainly concentrated in two swarm type sequences following above-average rainfall in March and August. For the first time, these data allow a detailed analysis of the activity in this rare example of an isolated but critical system.

[4] The observed seismicity is inconspicuous in its magnitude-frequency distribution that follows the Gutenberg-Richter law with a typical  $b$ -value of  $1.1 \pm 0.1$  for magnitudes larger than  $M_l = -0.2$ . Below this value the distribution deviates from the Gutenberg-Richter law, indicating incomplete data collection. We therefore restrict our analysis to  $M_l \geq -0.2$  events. Hypocenter locations are derived for a subset of these events using a 2D-velocity model with topography. Groups of events with very similar wave forms are identified by cluster analysis and relocated using the master event technique [Kraft et al., 2006b]. In this way, over 500 locations were obtained, shown as points in Figure 1.

### 3. Seismicity Model

[5] In order to test the hypothesis that rainfall triggered seismicity, we calculate the pore-fluid pressure changes at depth in response to the surface rain. Assuming a homogeneous crust and spatially uniform rainfall, we can restrict our analysis to the one-dimensional case. The process of fluid pressure relaxation can be approximately characterized by a system of equations describing the dynamics of fluid saturated porous elastic solid [Biot, 1962]. A diffusion equation describing the evolution of fluid mass alteration per unit volume,  $m$ , can be uncoupled [Rudnicki, 1986; PHASE Research Project, 2005]

$$\frac{\partial m}{\partial t} = D \frac{\partial^2 m}{\partial z^2} + Q(z, t), \quad (1)$$

where  $z$  is the depth coordinate,  $D$  the hydraulic diffusivity, and  $Q(z, t)$  a fluid mass source. If porosity is assumed to be

<sup>1</sup>Institute of Geosciences, University of Potsdam, Potsdam, Germany.

<sup>2</sup>Department of Earth and Environmental Sciences, Ludwig-Maximilians-University, Munich, Germany.

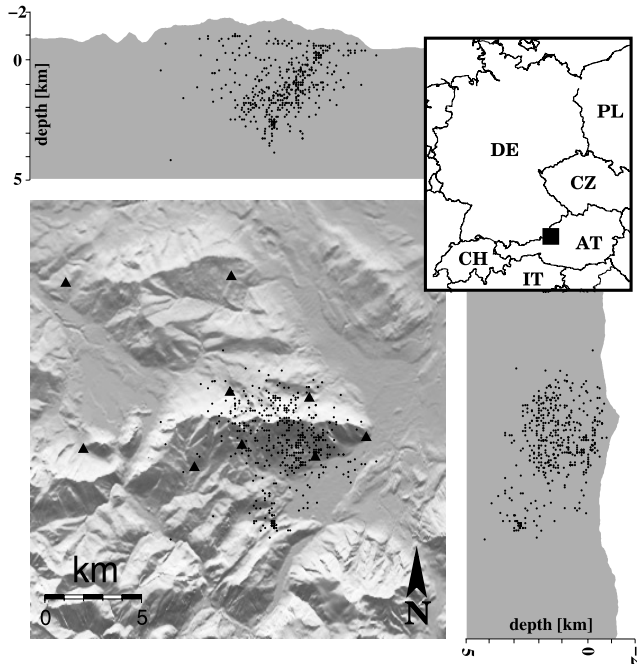


**Figure 1.** Map of Staufen Massif as well as EW and NS profiles through the summit of Mt. Hochstaufen (1775m) with the located earthquakes in the year 2002 (dots). Map borders are longitude  $12^{\circ}40' - 12^{\circ}57' E$  and latitude  $47^{\circ}40.5' - 47^{\circ}55.5' N$ . Triangles mark seismological stations installed in 2002.

constant, the alteration of pore pressure  $p$  is proportional to the mass alteration  $m$  and the same equation holds for the pore pressure alteration where  $Q(z,t)$  now defines the pressure source. The solution of the diffusion equation is given by

$$p(z,t) = \int_{-\infty}^t \int_{-\infty}^{\infty} 2G(z-z_0, t-\tau) Q(z_0, \tau) dz_0 d\tau \quad (2)$$

with Green's function  $G(z-z_0, t-\tau) = [4\pi D (t-\tau)]^{-0.5} \exp[-(z-z_0)^2/4 D (t-\tau)]$  [Barton, 1989]. The factor of 2 results from the fact that the total fluid mass which can only migrate into depth must be conserved [Landau and Lifschitz, 1966]. In our case, the source is given by the linearly interpolated rain rate measured at four daily sampled meteorologic stations surrounding Mt. Hochstaufen. Because we are only interested in pressure deviations from the stationary state, we consider the deviation of the rainfall from the long-term mean, namely  $Q(z,t) = \rho g (h(t) - \bar{h}) \delta(z)$ . The average rain amount  $\bar{h}$  is calculated from the precipitation data from 1995–2001 at the same meteorological stations. To avoid boundary effects, we start the integration of equation (2) at 1/1/2001.

[6] To quantify the effect of the pressure changes on seismicity, we use the framework of rate-state friction [Dieterich, 1994; Dieterich et al., 2000] which properly takes into consideration the rate- and slip-dependence of frictional strength and time-dependent restrengthening observed in laboratory experiments. This concept has already been successfully applied to explain earthquake clustering

in nature such as aftershock activity [Scholz, 1998]. In this theory, the seismicity rate  $\lambda$  is inversely proportional to the state variable  $\gamma$  describing the creep velocities on the faults, namely  $\lambda(z,t) = r/(\dot{\tau} \gamma(z,t))$ , where  $r$  is the stationary background rate and  $\dot{\tau}$  the tectonic loading rate. The evolution of the state variable is given by  $d\gamma = (dt - \gamma dCFS)/(A\sigma)$  with  $A$  being a dimensionless fault constitutive parameter usually  $\sim 0.01$  [Dieterich, 1994; Dieterich et al., 2000]. In our case, the Coulomb failure stress  $CFS$  changes due the constant stressing rate  $\dot{\tau}$  and the variation of the pore pressure  $p$ , altering the effective normal stress  $\sigma = \sigma_n - p$  on the faults. We track the evolution of  $\gamma$  by considering sufficiently small time steps leading to stress increments of  $\Delta CFS(z,t) = \dot{\tau} \Delta t + \mu(p(z,t+\Delta t) - p(z,t))$ . We choose time steps of 0.5 days and set the coefficient of friction  $\mu$  to the typical value of 0.6 [Byerlee, 1978]. The state variable is iterated according to

$$\dot{\tau} \gamma(z, t + \Delta t) = \dot{\tau} \gamma(z, t) e^{-\frac{\Delta CFS}{A\sigma}} + \frac{\Delta t}{t_a} \quad (3)$$

starting from the background level, that is,  $\dot{\tau} \gamma(z, 0) = 1$ . Because the pressure changes are assumed to be much smaller than the effective normal stress, we can use  $A\sigma$  as a constant free parameter. The rate depends additionally on the value of the background rate  $r$ , the relaxation time  $t_a = A\sigma/\dot{\tau}$ , and implicitly on the hydraulic diffusivity  $D$ .

#### 4. Results

[7] The estimation of the four parameters is carried out by the maximum likelihood method. The likelihood function  $L$ , which is the joint probability function for a given model, is constructed by multiplying the probability density function of each of the data points together. For a given rate  $\lambda(z,t)$ , the log-likelihood with respect to the  $N$  earthquakes occurring at the depth interval  $[z_0, z_1]$  at times  $t_i$  can be determined by

$$\ln L(r, t_a, A\sigma, D) = \sum_{i=1}^N \ln \lambda(z_i, t_i) - \int_{t_s}^{t_e} \int_{z_0}^{z_1} \lambda(z, t) dz dt, \quad (4)$$

where  $t_s = 1/1/2002$  is the starting and  $t_e = 1/1/2003$  the ending time of the activity [Ogata, 1998; Daley and Vere-Jones, 2003]. We account for the uncertainty of earthquake locations by evaluating the formula (4) for  $z_i$  which are Gaussian distributed around the determined values. According to the localization procedure, the location errors vary between 50m and 2km with a median of 200m.

[8] For the earthquakes in the depth interval 1–4 km, the result of the parameter grid-search is illustrated in Figure 2. The maximization of the likelihood function (equation 4) yields  $r = 0.45 \pm 0.05$  [days<sup>-1</sup>],  $t_a = 180 \pm 60$  [days],  $A\sigma = 110 \pm 10$  [Pa] and a hydraulic diffusivity  $D = 3.3 \pm 0.8$  m<sup>2</sup>/s, where the errors refer to a 63%-decrease of the likelihood function. Considering a typical value of  $A = 0.01$ , our estimated  $A\sigma$ -value would yield an effective normal stress of only 11 [kPa] which requires very high in situ pore pressure in this region (see further discussion in section 5). The resulting diffusivity value, which corresponds well to the range of values obtained from fluid injection experi-

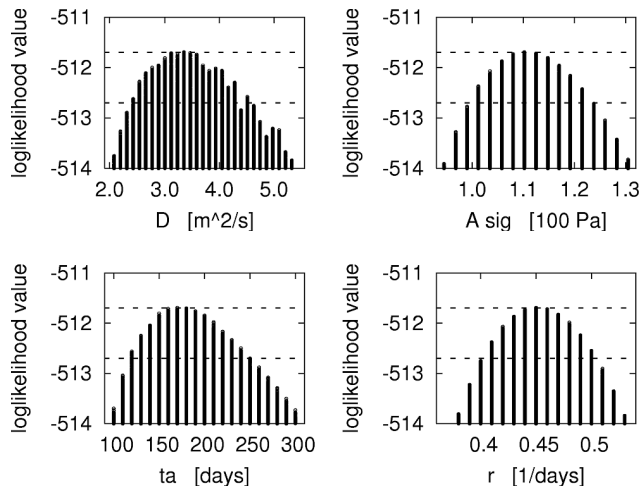


**Figure 2.** The result of the parameter search for maximizing the likelihood value. Additionally, the maximum as well as the 63% decrease of the likelihood value are plotted as horizontal lines.

ments [e.g., Shapiro *et al.*, 1997], is slightly higher than the previously estimated value for the same region of  $0.75 \pm 0.35 \text{ m}^2/\text{s}$  [Kraft *et al.*, 2006a]. However, the previous result is based only on fitting single pressure-front curves to first locations of the observed activity and did not incorporate the complete pressure field. Using our estimated value for hydraulic diffusivity, we calculate now the pore pressure variations at depth from the observed rainfall (Figure 3a). The comparison of the observed seismic activity with the resulting spatio-temporal pressure field is shown in Figure 3b and with the forecasted earthquake rate in Figure 3c. In either case, the observed seismicity (indicated by stars) corresponds well to elevated values of the calculated functions, indicating a strong spatial and temporal correlation. In Figure 3d, the calculated and observed earthquake rate, including also the events without hypocenter information ( $M_l \geq -0.2$ ), are compared in the form of time series representing the number of earthquakes per day. The correlation between these time series and between those of observed earthquake rate and rainfall is quantified by their cross-correlation coefficient, shown in Figure 4. While the seismicity is not correlated with the rain data at zero time delay, it shows some correlation if the seismicity is shifted backwards 8 days ( $R_{\text{max}} = 0.47$ ). On the other hand, the earthquake rate calculated from the pore pressure changes at depth is strongly correlated at zero delay time with a maximum correlation coefficient, almost doubling that of the rain data ( $R_{\text{max}} = 0.82$ ). Note that the value of the hydraulic diffusivity that maximizes the likelihood function in equation (4), is also found to maximize the linear correlation coefficient indicating the consistency of our parameter estimation.

## 5. Discussion

[9] The high correlation indicates that our model is a good approximation of the underlying processes, although we have strongly simplified the real world. In particular, the crust is assumed to be a homogeneous half-space which

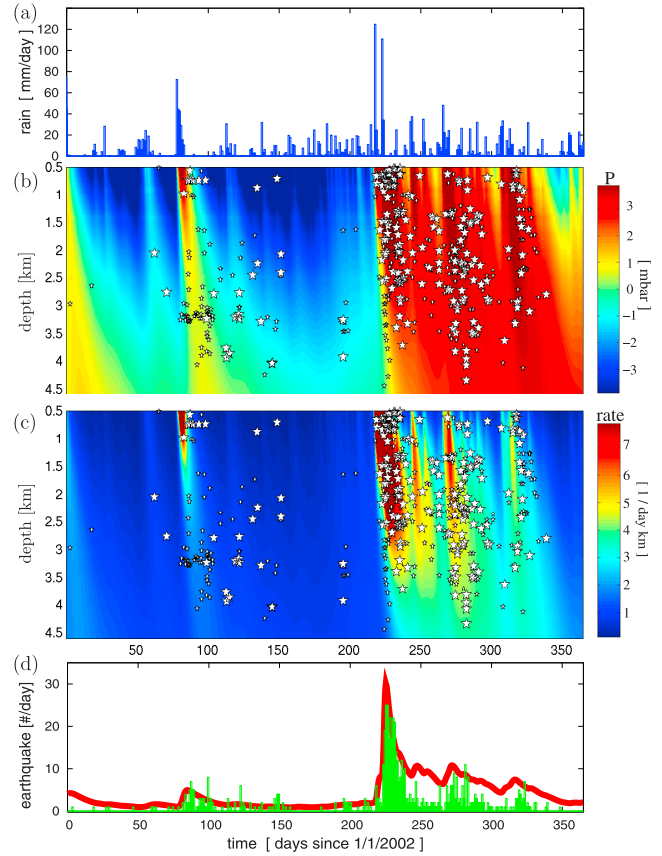


**Figure 3.** The spatiotemporal pattern of (b) pore pressure and (c) estimated earthquake rate as the result of the surface rain rate (a) in the case of one-dimensional linear diffusion with hydraulic diffusivity  $D = 3.3 \text{ m}^2/\text{s}^2$ . Earthquake locations are marked by white stars (big: errors  $\leq 100\text{m}$ ). (d) The daily number of detected earthquakes (green) in comparison with the theoretical rate for the 1–4 km depth interval (red).

certainly is an over-simplified model of the local geology, where systems of open fractures are observed [Weede, 2002] extending from the surface to depth of at least 100m. Thus a likely situation is a localized channeling of larger volume of

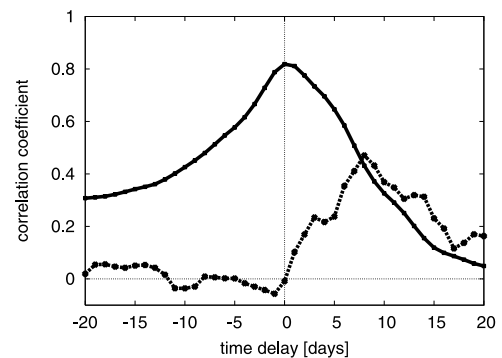


**Figure 4.** The linear correlation coefficient as a function of the time shift between the time series of the daily observed number of earthquakes and (1) the daily rain amount (dashed line) and (2) the theoretical rate of earthquakes in the 1–4 km depth interval (solid line).



precipitation into a limited number of open fractures, resulting in strongly amplified hydraulic head changes. If fluid diffusion is assumed to be confined within deep fracture zones, the physics of rate-state friction and fluid pressure diffusion within an equivalent porous medium model [e.g., Berkowitz *et al.*, 1988] would be the same. The only effect would be that the estimated value of the parameter  $A\sigma$  would be amplified in the same way as the pressure, because the evolution of the state variable  $\hat{\tau} \gamma$  (equation 3) is invariant under identical amplification of  $p$ ,  $\hat{\tau}$ , and  $A\sigma$ .

[10] Furthermore, we have neglected in our model seasonal effects such as snow coverage as well as coseismic stress changes induced by the earthquakes themselves, which are known to trigger local aftershocks according to the Omori law [Stein, 1999]. Previous studies of natural swarm activity in the Vogtland region, Central Europe, indicate that aftershock sequences are embedded in the swarm activity and can even dominate it [Hainzl and Ogata, 2005]. However, for the Mt. Hochstaufen region, simple stacking of the activity relative to the largest events indicates that aftershocks play only a minor role.

[11] Assuming homogeneous conditions, the absolute pressure variation during the year is found to be between 0.5 – 1.3 kPa in the depth range between 1–4 km, where most of the earthquakes occurred. This is in the same range as the effects of earth tides [Tolstoy *et al.*, 2002]. However, inserting tidal stresses (calculated from volume strain at 2 km depth below Bad Reichenhall) as the loading mechanism into our model yields a maximum effect of only 15% compared to the rainfall induced rate changes. The underlying reason is the higher frequency of the tidal stress changes. The relative effect of tides would be further reduced in the likely case that rain is collected in open fracture systems at the surface (see above).

## 6. Conclusions

[12] Although some seasonal variability of seismicity related to ground water recharge and precipitation has been previously observed [Saar and Manga, 2003; Muco, 1999], we can show here for the first time a statistically significant causal relationship between rainfall and earthquake activity for an isolated region. Our analysis of the high quality meteorological and seismic data in the Mt. Hochstaufen region yields clear evidence that pore pressure changes induced by rainfall are able to trigger earthquake activity even at 4 km depth via the mechanism of fluid diffusion. Assuming homogeneous condition, stress changes of the order of millibar are found to trigger the earthquakes. This is much less than usually observed for the bulk of induced earthquakes in fluid injection experiments (in the order of 10 bar), even though some fraction of those events has been triggered by similar tiny pressure changes [Zoback and Harjes, 1997; PHASE Research Project, 2005]. Our results indicate an extreme sensitivity of the crust with regard to minute changes. However, the existence of deep open faults channeling larger volume of precipitation would lead to significantly higher stress changes which could explain the sensitivity of the seismogenic volume in the Mt. Hochstaufen region. In any case, the high

correlation between rain-induced pressure changes at depth and seismicity opens the possibility of forecasting future earthquake rates on the basis of rainfall data in this region.

[13] **Acknowledgments.** The authors want to thank Serge Shapiro and two anonymous reviewers for their fruitful comments as well as Jim Dieterich and Agnes Helmstetter for helpful discussion of the rate-state friction framework. Furthermore, we are thankful to Thomas Jahr for calculating the tidal effects and Ed Sobel for carefully reading the manuscript. This work was supported by the Deutsche Forschungsgemeinschaft (SCHE280/14-2 and Ig16/7), Bavarian Ministry for Environment, and the EU Community initiative INTERREG III B Alpine Space Programme SISMOVALP.

## References

- Barton, G. (1989), *Elements of Green's Functions and Propagation: Potentials, Diffusion and Waves*, Oxford Univ. Press, New York.
- Berkowitz, B., J. Bear, and C. Braester (1988), Continuum models for contaminant transport in fractured porous formations, *Water Resour. Res.*, *24*, 1225–1236.
- Biot, M. (1962), Mechanics of deformation and acoustic propagation in porous media, *J. Appl. Phys.*, *33*, 1482–1498.
- Bögel, H., and K. Schmidt (1976), *Kleine Geologie der Ostalpen*, Ott Verlag, Thun, Switzerland.
- Byerlee, J. D. (1978), Friction of rocks, *Pure Appl. Geophys.*, *116*, 615–629.
- Daley, D. J., and D. Vere-Jones (2003), *An Introduction to the Theory of Point Processes*, vol. 1, *Elementary Theory and Methods*, 2nd ed., Springer, New York.
- Dieterich, J. H. (1994), A constitutive law for rate of earthquake production and its application to earthquake clustering, *J. Geophys. Res.*, *99*, 2601–2618.
- Dieterich, J. H., V. Cayol, and P. Okubo (2000), The use of earthquake rate changes as a stress meter at Kilauea volcano, *Nature*, *408*, 457–460.
- Hainzl, S., and Y. Ogata (2005), Detecting fluid signals in seismicity data through statistical earthquake modeling, *J. Geophys. Res.*, *110*, B05S07, doi:10.1029/2004JB003247.
- Kodaira, S., T. Idaka, A. Kato, J. Park, and Y. Kaneda (2004), High pore pressure may cause silent slip in the Nankai Through, *Science*, *304*, 1295–1298.
- Kraft, T., J. Wassermann, E. Schmedes, and H. Igel (2006a), Meteorological triggering of earthquake swarms at Mt. Hochstaufen, SE-Germany, *Tectonophysics*, *424*, 245–258.
- Kraft, T., J. Wassermann, and H. Igel (2006b), High-precision relocation and focal mechanism determination of the 2002 rain-triggered earthquake swarm activity at Mt. Hochstaufen, SE-Germany, *Geophys. J. Int.*, in press.
- Landau, L. D., and E. M. Lifschitz (1966), *Lehrbuch der Theoretischen Physik VI*, Sect. 52, Akademie-Verlag, Berlin.
- Miller, S. A., C. Collettini, L. Chiaraluce, M. Cocco, M. Barchi, and B. J. P. Kaus (2004), Aftershocks driven by a high-pressure CO<sub>2</sub> source at depth, *Nature*, *427*, 724–727.
- Muco, B. (1999), Statistical investigation on possible seasonality of seismic activity and rainfall-induced earthquakes in Balkan area, *Phys. Earth Planet. Inter.*, *114*, 119–127.
- Nur, A., and J. Booker (1972), Aftershocks caused by pore fluid flow?, *Science*, *175*, 885–887.
- Ogata, Y. (1998), Space-time point-process models for earthquake occurrences, *Ann. Inst. Stat. Math.*, *50*, 379–402.
- Parotidis, M., E. Rother, and S. A. Shapiro (2003), Pore-pressure diffusion: A possible triggering mechanism for the earthquake swarms 2000 in Vogtland/NW-Bohemia, Central Europe, *Geophys. Res. Lett.*, *30*(20), 2075, doi:10.1029/2003GL018110.
- PHASE Research Project, (2005), Annual report, Freie Univ., Berlin. (Available at <http://phase.geophysik.fu-berlin.de/index.html>)
- Prejean, S. G., et al. (2004), Remotely triggered seismicity on the United States west coast following the Mw 7.9 Denali Fault earthquake, *Bull. Seismol. Soc. Am.*, *94*, 348–359.
- Rudnicki, J. W. (1986), Fluid mass sources and point forces in linear elastic diffusive solids, *Mech. Mater.*, *5*, 383–393.
- Saar, O., and M. Manga (2003), Seismicity induces by seasonal groundwater recharge at Mt. Hood, Oregon, *Earth Planet. Sci. Lett.*, *214*, 605–618.
- Scholz, C. H. (1998), Earthquakes and friction laws, *Nature*, *391*, 37–42.
- Shapiro, S. A., E. Huenges, and G. Borm (1997), Estimating the crust permeability from fluid-injection-induced seismic emission at the KTB site, *Geophys. J. Int.*, *131*, F15–F18.

- Sleep, N., and M. L. Blanpied (1992), Creep, compaction and the weak rheology of major faults, *Nature*, 359, 687–692.
- Stein, R. S. (1999), The role of stress transfer in earthquake occurrence, *Nature*, 402, 605–609.
- Talwani, P. (1997), On the nature of reservoir-induced seismicity, *Pure Appl. Geophys.*, 150, 473–492.
- Tolstoy, M., F. L. Vernon, J. A. Orcutt, and F. K. Wyatt (2002), The breathing of the seafloor: Tidal correlations of seismicity on Axial volcano, *Geology*, 30, 503–506.
- Weede, M. (2002), Die Geologie des Hochstaufen unter besonderer Berücksichtigung der Massenbewegungen, diploma thesis, Tech. Univ. of Munich, Munich, Germany.
- Zoback, M. D., and H.-P. Harjes (1997), Injection-induced earthquakes and crustal stress at 9 km depth at the KTB deep drilling site, Germany, *J. Geophys. Res.*, 102, 18,477–18,492.
- 
- S. Hainzl, Institute of Geosciences, University of Potsdam, POB 60 15 53, D-14415 Potsdam, Germany. (hainzl@geo.uni-potsdam.de)
- H. Igel, T. Kraft, E. Schmedes, and J. Wassermann, Department of Earth and Environmental Sciences, Ludwig-Maximilians-University, Theresienstrasse 41, D-80333 Munich, Germany. (heiner.igel@geophysik.uni-muenchen.de; toni@gfz-potsdam.de; eberhard.schmedes@geophysik.uni-muenchen.de; joachim.wassermann@geophysik.uni-muenchen.de)